Supplementary Information

Quasi-Honeycomb Graphene Architectures Enabling Geometry-Adaptive Thermal Regulation for High-Density Electronics

Qiang Zhao [a], Ying Wang [b], Xiang Zheng [a], Xianzhen Cai [c], Jingze Li [a], and Yongqi Zhang [c, *], Xinhui Xia [d, *]

[a] School of Materials and Energy, University of Electronic Science and Technology of China, Chengdu, 610054, Sichuan, China

[b] School of Electronic Science and Engineering, University of Electronic Science and Technology of China, Chengdu 610054, Sichuan, China

[c] Institute of Fundamental and Frontier Sciences, University of Electronic Science and Technology of China, Chengdu 610054, Sichuan, China

[d] College of Materials Science & Engineering, Zhejiang University of Technology, Hangzhou 310014, Zhejiang, China

Corresponding Author: Yongqi Zhang — Institute of Fundamental and Frontier Sciences, University of Electronic Science and Technology of China, Chengdu 610054, Sichuan; China
E-mail: yqzhang@uestc.edu.cn

Note S1 A combined experimental and simulation-based method for determining the net heat flux and the convective heat transfer coefficient.

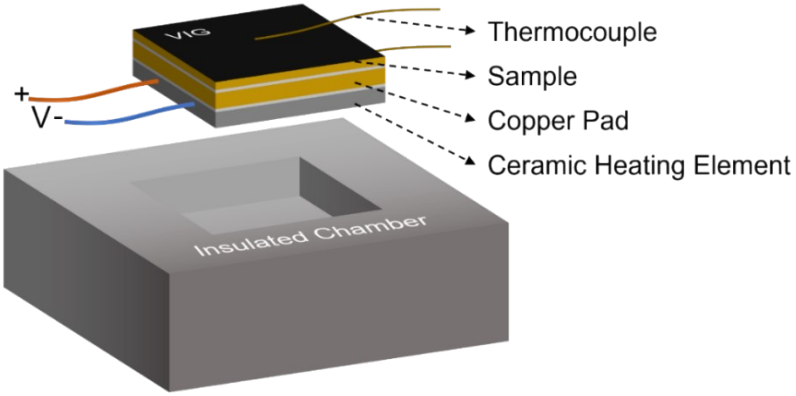

Figure S1. The schematic diagram of the heat dissipation performance test assembly.

Precisely acquiring the net heat flux exchanged to the environment from the sample surface is of essential for accurately determining the thermal parameters of the heat dissipation surface. In our experiment, despite the thermal conduction channel being surrounded by materials with extremely low thermal conductivity, the temperature gradient still induced heat leakage from surfaces other than the sample surface. To obtain the net heat flux exchanged from the sample surface to the environment, the surface temperature and emissivity of the sample were first measured under a constant heat source power. The surface temperature was determined using thermocouples attached to the sample surface. The surface emissivity was determined by synchronously measuring the temperature using thermocouples and an infrared thermometer positioned above the surface[[1, 2]]. Then, a fully equivalent model was constructed and simulated using COMSOL Multiphysics® software. Given that the input power, surface temperature, and surface emissivity are known quantities, the only remaining unknown is the convective heat transfer coefficient of the sample surface. Consequently, by conducting a parametric scanning process to match the observed surface temperature values, we can accurately determine both the convective heat transfer coefficient of the sample surface and the net heat flux exchanged from the sample surface to the environment.

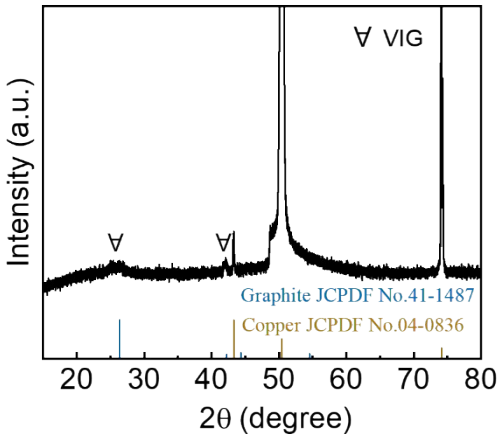

Figure S2. XRD pattern of the VIG/Cu sample.

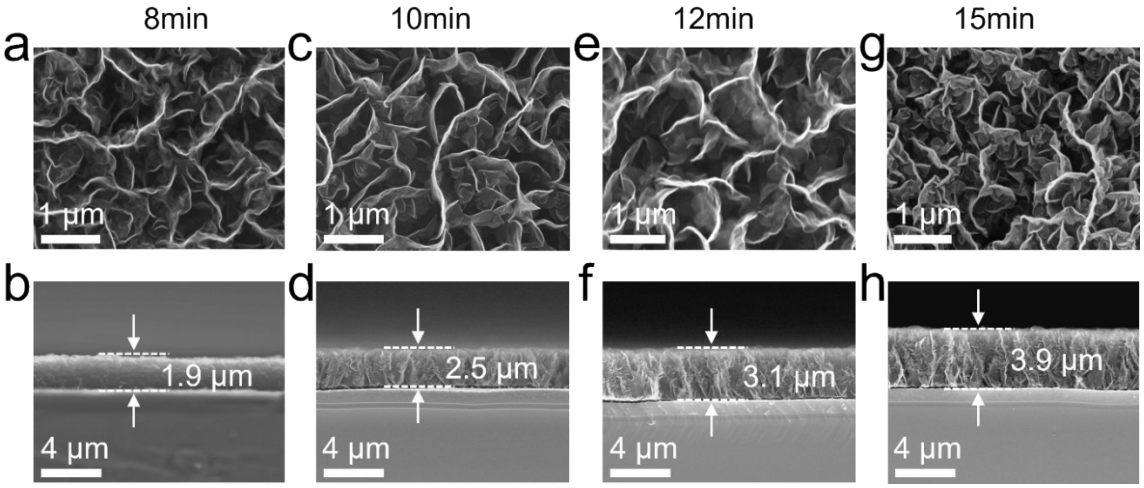

Figure S3. The surface and cross-sectional micrographs of VIG with varying growth durations of 8 min (a and b), 10 min (c and d), 12 min (e and f) and 15 min (g and h).

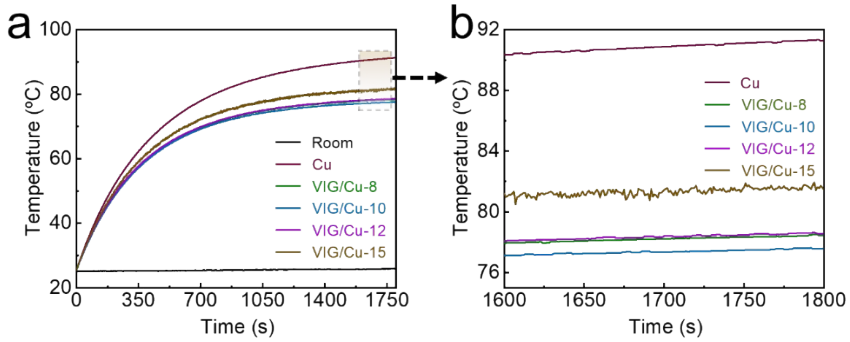

Figure S4. Time evolution curves of the temperature of heat source at a power density of 0.23 W/cm^{-2}, using bare copper and VIG with various thicknesses as cooling surfaces.

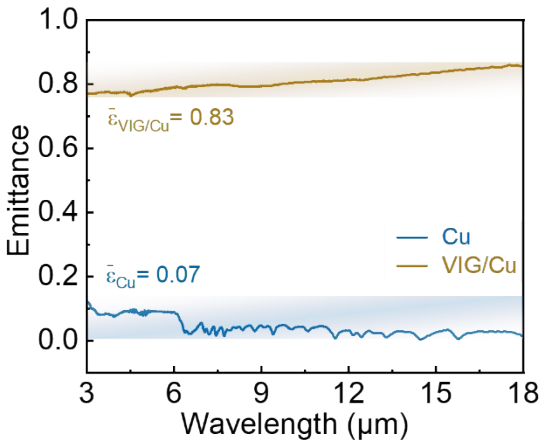

Figure S5. Emittance spectra of VIG/Cu and bare Cu surfaces from 3 μm to 18 μm.

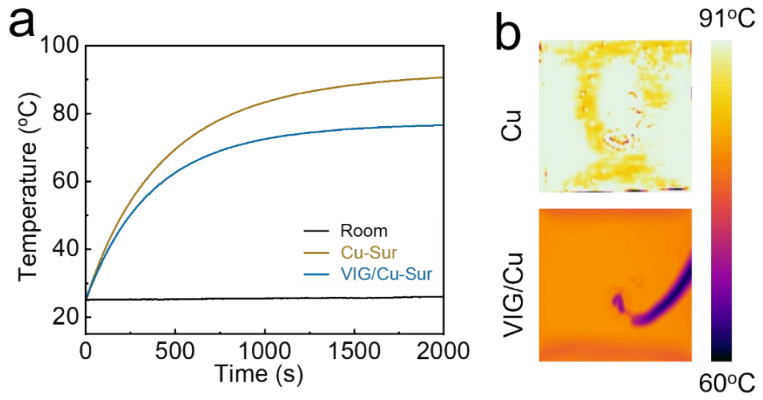

Figure S6. (a) The surface temperature-time evolution curves of bare Cu and VIG/Cu surfaces. (b) The infrared images of bare Cu and VIG/Cu surfaces at steady-state.

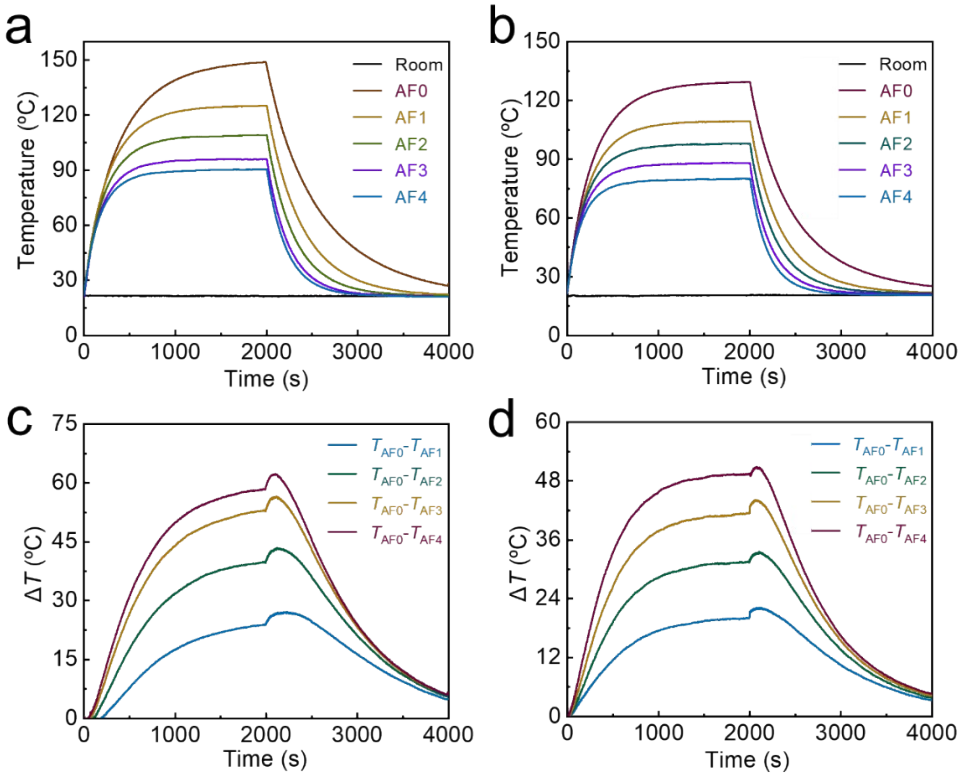

Figure S7. The time evolution curves of the heat source temperature using Cu (a) and VIG/Cu (b) as cooling surfaces under various airflow conditions. (c) The temperature difference of the heat source between zero airflow condition and other airflow conditions when bare Cu was used as the cooling surface. (d) The temperature difference of the heat source between zero airflow condition and other airflow conditions when VIG/Cu was used as the cooling surface.

Note S2

The experimental setup replicated passive cooling configurations (Figure 2e), with the critical addition of a fan positioned 5 mm above the heat dissipation surface to generate airflow rates spanning 0–23.53 CFM (AF0 = 0 CFM, AF1 = 6.12 CFM, AF2 = 12.24 CFM, AF3 = 18.09 CFM and AF4 = 23.53 CFM). The surface temperature of the sample and the ambient temperature were measured using two K-type thermocouples. The total power of the heat source was supplied by a DC power supply. The net heat flux (P) was determined as described in Note S1. The airflow velocity was measured using a digital anemometer. The effective heat transfer coefficient (H) was calculated using the following equation:

$$H = \frac{P}{A(T_s - T_a)} \tag{S1}$$

where P is the net heat flux exchanged with the environment through the sample surfaces (which was calculated using a combination of simulation methods with the model in Figure S1 and experimental data), A is the projected surface area of the sample (in cm²), T_s is the steady-state surface temperature of the sample (measured via K-type thermocouple), and T_a is the ambient temperature (maintained at ~25°C in our controlled chamber).

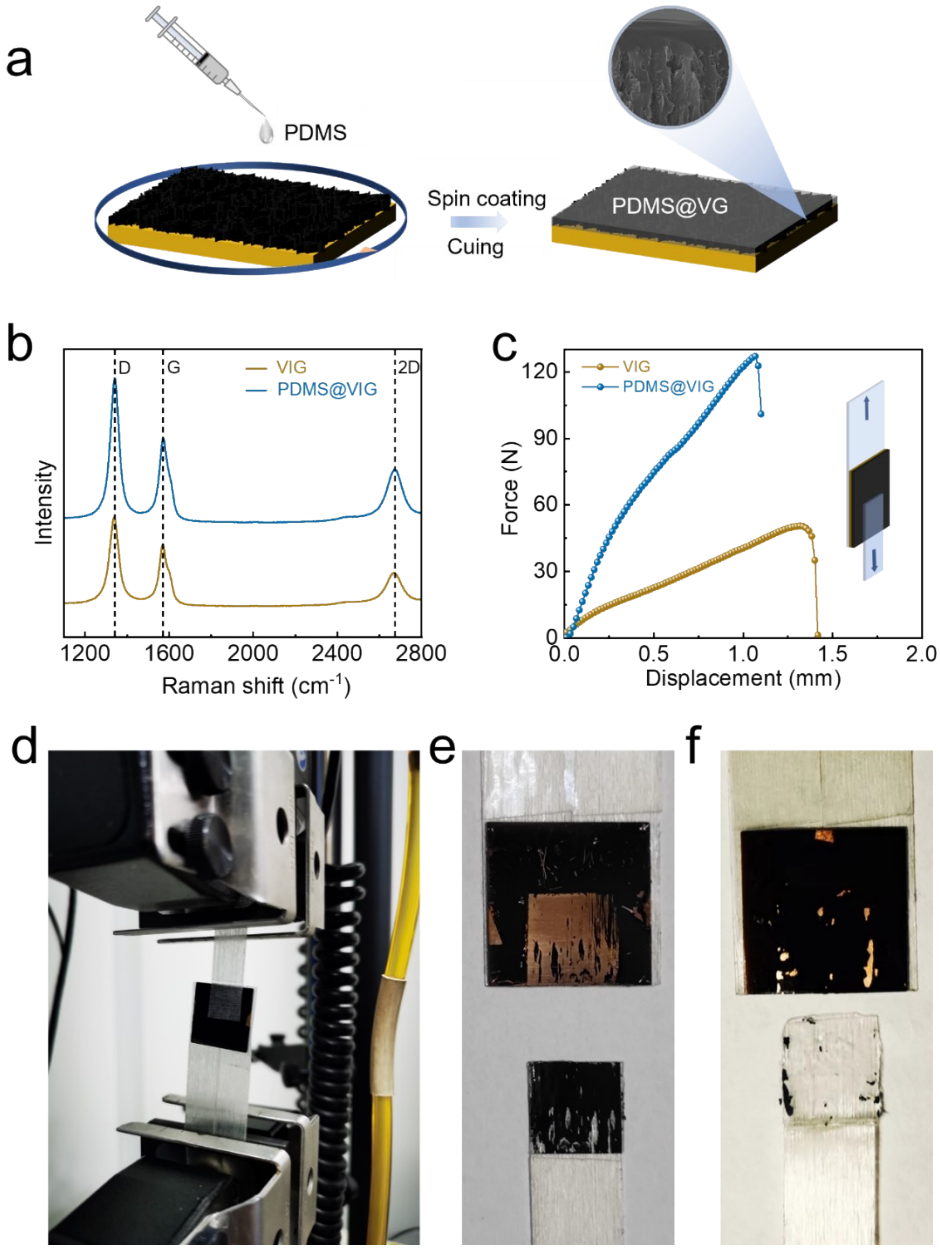

Figure S8. (a) Schematic of the PDMS filling Process. (b)The Raman spectra of the VIG and PDMS@VIG. (c) The force-displacement curves of VIG and PDMS@VIG vs. the fiber tape. (d) On-site photograph of the peeling test for the VIG/Cu sample. (e) and (f) Optical photographs of the VIG/Cu and PDMS@VIG/Cu samples after the peeling test.

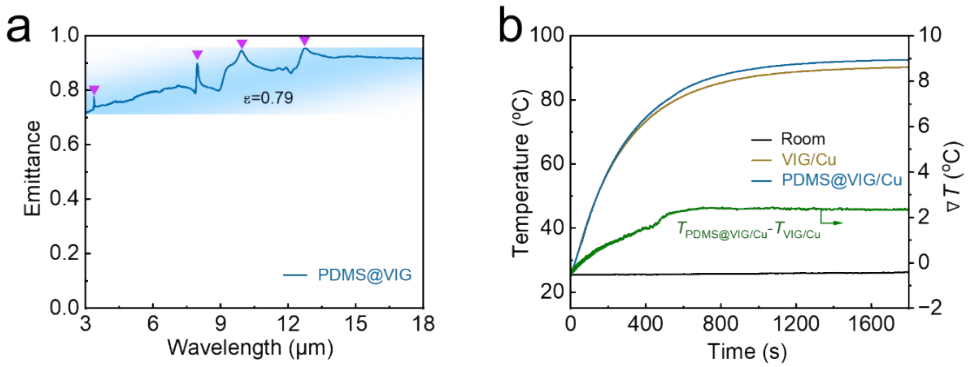

Figure S9. (a) Emittance spectra of PDMS@VIG from 3 μm to 18 μm. (b) Evolution of the heat source temperature with VIG/Cu and PDMS@VIG/Cu as heat sinks.

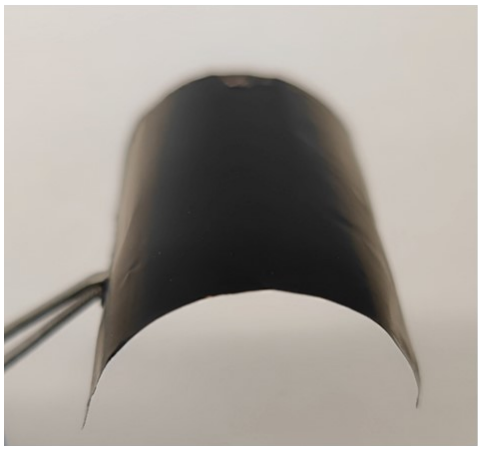

Figure S10. Optical photograph of the geometry-adaptive VIG/Cu structure.

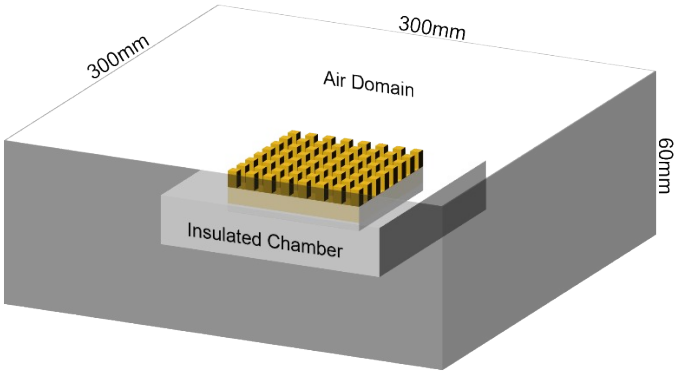

Figure S11. Schematic illustration of the coupled solid–fluid heat transfer simulation model.

Note S3

A schematic of the coupled solid–fluid heat dissipation model is shown in Figure S11, and the corresponding material parameters are listed in Table S2. Specifically, the experimental setup illustrated in Figure S1 was surrounded by an air domain with dimensions of 300 mm × 300 mm × 60 mm. The bottom surfaces of both the insulated chamber and the air domain were defined as adiabatic boundaries, while the other five sides of the air domain were set as open boundaries to allow buoyancy-driven airflow. The internal surfaces of the copper-fin heat sink were assigned surface-to-surface radiation boundary conditions, and the external surfaces were set with surface-to-ambient radiation boundaries. Air was modeled as a weakly compressible fluid including gravitational effects, with an initial pressure of 1 atm. A steady-state solver with adaptive meshing was used to ensure convergence. The height of the copper fins was parameterized to determine the configuration consistent with the heat dissipation performance of the VIG structure.

Table S2 Material properties of the simulation model. density (ρ), specific heat capacity (C_p), thermal conductivity (k) and dynamic viscosity (μ)

Material	ρ (g cm^{-3})	C_p (J g^{-1} k^{-1})	k (W m^{-1} K^{-1})	μ (Pa s)
Air	1.16×10^{-3}	1.006	0.026	1.86×10^{-5}
Copper	8.96	0.385	380	/
Alumina	3.9	0.9	27	/
Insulated chamber	0.41	0.703	0.02	/

References

[1] G. Zhang, S.H. Jiang, W. Yao, C.H. Liu, Enhancement of Natural Convection by Carbon Nanotube Films Covered Microchannel-Surface for Passive Electronic Cooling Devices, ACS Appl. Mater. Interfaces 8 (2016) 31202-31211.

[2] C.N. Suryawanshi, T. Kim, C.T. Lin, An instrument for evaluation of performance of heat dissipative coatings, Rev. Sci. Instrum. 81 (2010) 6.